Numerical analysis of two-layer beams with interlayer slip and step-wise linear interface law

Ilaria Monetto and Francesca Campi

DICCA – Department of Civil, Chemical and Environmental Engineering, University of Genoa,
Via Montallegro 1, 16145 Genova, Italy

Abstract

Progressive interface failure in two-layer beams with partial shear connection is simulated. The mathematical model, based on classical beam theories and linear non-proportional interface laws, proposed previously by the authors, is considered. The related fundamental analytical solution is rewritten in vector form to facilitate the determination of the high number of arbitrary constants on which the general solution for a generic configuration of the composite beam, characterized by different regimes coexisting along the interface, depends. This is employed in the simulation of a process of progressive interface debonding as a sequence of equilibrated consecutive configurations assumed by the composite beam. Numerical analyses are finally performed to validate the solution procedure proposed.

Keywords: two-layer beam; interlayer slip; nonlinear interface.

1. Introduction

Composite systems consisting of two structural elements connected together at the common interface are widely used in many practical applications. Steel – concrete beams and wood, concrete or steel elements (beams, arches, vaults, etc) repaired with steel plates or fiber composite strips are common in civil engineering applications. In such systems, the chemical or mechanical bond established by means of adhesive interlayers or shear connectors forces the two parts to act together as a composite so improving the global stiffness, strength and toughness.

The nature of the bond strongly affects the interaction between the two elements and the mechanical behavior of the composite, as a consequence. A perfect composite action, resulting in a complete transmission of both normal and shear stresses between the two elements, can be obtained by preventing that relative displacements occur at the common interface. However, because of the deformability of the bond system, this can hardly be obtained in practice so that the two elements

usually interact only partially and slips and/or uplifts at the common interface may develop. Furthermore, the mechanical properties of the connection can vary during the loading history as a consequence of the initiation and propagation of decohesion zones at the interface. Such a process leads to a further reduction of the degree of composite action and of the global stiffness and strength of the system, as a consequence, leading to its failure even if each element behaves elastically.

The optimal design of composite systems then requires the development of a better understanding of their mechanical response depending on the evolution of the degree of composite action between the elements during the loading history. In order to do this, simplified analytical models, which provide explicit solutions, are preferable to numerical analyses, related to prescribed geometry, material properties and interface constitutive behavior. This permits one to perform parametric analyses and then investigate the effects of model parameters on the global response of such systems.

Within this context, a large number of works exists on the problem of two-layer composite beams with an imperfect interface, so guaranteeing only a partial composite action, assumed to exhibit a linear elastic mechanical behavior. Most of these works build on the theory developed by Newmark et al. (1951) for steel – concrete beams with shear connections in the form of short pieces of reinforcing bars welded to the top flange of the steel element and embedded in the concrete. The model considers two linear elastic Euler-Bernoulli beams that undergo equal deflections but can slip one on the other in the longitudinal direction and assumes interlayer slips related to shear stresses transferred from one element to the other along their common interface according to a linear constitutive law. The subsequent analogous theories differ in some additional assumptions but result in similar governing equations. In particular, several exact solutions for simply supported beams subjected to different loading conditions were obtained (see e.g. Girhammar and Gopu, 1993; Cosenza and Mazzolani, 1993; Girhammar and Pan, 2007). Schnabl et al. (2007) took into account the effects of shear deformation on the equilibrium of the two elements modelled as linear elastic Timoshenko beams and proposed an algorithm to derive analytical solutions for prescribed boundary conditions. Xu and Wu (2007) presented an analogous theory and obtained analytical solutions for simple beams subjected to uniformly distributed loads and under different boundary conditions. Other analytical solutions for two-layer composite beams consisting of two elements which can undergo relative displacements in both the longitudinal and transversal directions exist on the basis of both linear elastic Euler-Bernoulli (Wang, 2006) or Timoshenko (Qiao and Wang, 2005; Bennati et al., 2009) beam theory.

However, only a little attention has been focused on the nonlinear interfacial behavior due, for example, to progressive damage and failure of the connection or to yielding of connectors during the loading history (Wheat, 1994; Wang, 2006; Hozjan et al., 2013). Among the others, Cas et al.

(2004) proposed a new finite element model to study composite beams with interlayer slip and validated the model with comparison with experimental results of full-scale laboratory tests. In particular they analyzed the behavior of a composite beam made of a reinforced concrete slab and steel girder connected to each other with steel shear studs. The proposed method is capable of modelling both continuous and discrete connectors. Battini et al. (2009) first proposed a numerical formulation for the analysis of two-layer composite plane beams with interlayer slips, based on the derivation of the exact stiffness matrix. More recently, Campi and Monetto (2013) proposed a new formulation for the problem of partial interaction in two-layer beams undergoing interlayer slips based on a linear non-proportional description of the interfacial behavior. This formulation led to explicit expressions having general validity independently of the interface regime for all static and kinematic variables of the problem within both linear elastic Timoshenko and, as a special case, Euler-Bernoulli beam theories. This fundamental solution was employed in the analysis of two-layer beams with interlayer slip and bi-linear interface law for different boundary and loading conditions. Baraldi et al. (2016) proposed a discrete element model to investigate the post-breakage behavior of laminated glass structures where the interface is modelled as elasto-plastic.

This paper deals with the employment of the fundamental solution derived by Campi and Monetto (2013) to a wider class of nonlinear interfacial behaviors conveniently approximated through step-wise linear laws. This choice, supported by the comparison of experimental and numerical studies and previously made by many authors working on similar problems (Schreyer and Peffer, 2000; Lu et al., 2005; Wang, 2006), permits one to assume valid a priori the fundamental solution for each linear branch. The aim of this work is to simulate the response of composite beams for prescribed boundary conditions and loading history inducing a progressive debonding of the interface with a view towards an optimal design of the joint. In order to do this, the debonding process is analyzed as a sequence of different configurations of the composite beam in which adjacent portions of the interface experience different interfacial regimes according to the interfacial law under consideration. The general solution of the problem of equilibrium consists of as many sets of fundamental solutions as the number of interface portions. It is straightforward that, even considering a low number of regimes coexisting along the interface, this general solution depends on a high number of arbitrary constants. Furthermore, since the length of each interface portion depends on the level of load and then is unknown a priori, the problem is nonlinear. For bi-linear approximations of nonlinear interfacial behaviors Campi and Monetto (2013) adopted incremental calculation procedures. Here, more complicated approximations are considered, then incremental-iterative calculation procedures are followed to determine all such arbitrary constants.

The paper is organized as follows. Section 2 gives a brief statement of the main points of the model formulation and fundamental solution detailed in Campi and Monetto (2013). In Section 3

this solution is first rewritten in vector form and then employed to solve the equilibrium problem for a generic configuration of the composite beam. Such a vector form is also employed to derive the exact stiffness matrix and nodal force vector for a partially connected two-layer beam finite element, as detailed in Appendix B. Finally, Section 4 shows two sets of numerical results: i) a comparison with results found in literature to validate the employment of the fundamental closed form solution to practical applications; ii) the simulation of progressive debonding of the interface in two-layer beams with partial composite action. Section 5 concludes the paper with a summary and a final discussion of the advances, possible extensions and related limits of the formulation proposed.

2. Analytical model and fundamental solution

2.1 Model assumptions

The composite beam under consideration consists of two layers connected by a continuous bond. The layers have constant cross sections and are made of linearly elastic and homogeneous materials. The bond is perfect in the transverse direction, while ensures a partial composite action in the longitudinal direction. As a consequence, only interlayer slips are allowed at the interface, whereas no separation or interpenetration between the layers is possible. Figure 1 shows the undeformed and typical deformed configurations of the two-layer beam under consideration.

Under the assumption of small strains, displacements and rotations, each layer is modelled as a linearly elastic Timoshenko beam. The connection is modelled by continuously distributed normal and tangential reactions, the latter related to interlayer slips according to a suitable relationship, as discussed next. The two-layer beam is then subjected to the action of distributed loads and related internal forces and interfacial tractions. The reference structure is shown in Figure 2.

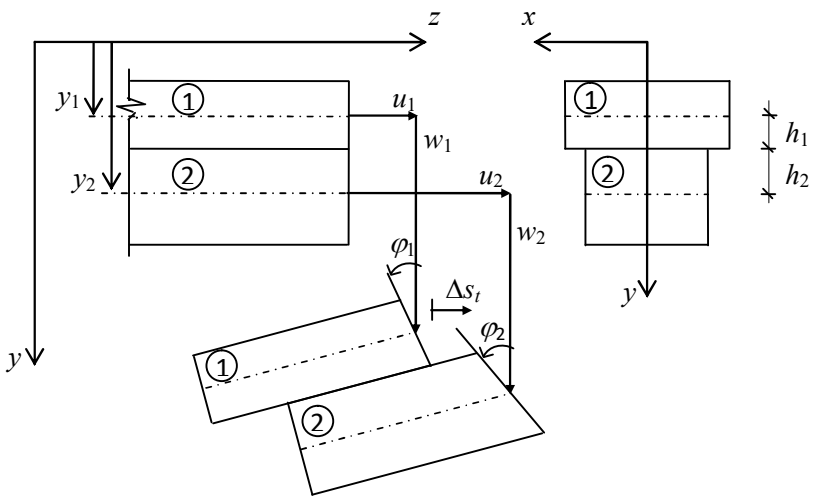

Figure 1. Geometry and deformed configuration of the two-layer beam.

2.2 Governing equations

The problem of the equilibrium of the composite beam under consideration is governed by the compatibility, equilibrium and constitutive equations for the two layers together with the bond conditions at the interface. In particular: (i) the assumption of perfect connection in the transverse direction y imposes that the two layers undergo equal deflections; (ii) according to Campi and Monetto (2013), the partial composite action in the longitudinal direction z is assumed to be described through the following linear non-proportional relationship between interlayer shear traction, say p_t, and slip, say Δs_t, at the interface (Figure 3):

$$p_t = A\,\Delta s_t + B = A\,(u_2 - u_1 - h_1\varphi_1 - h_2\varphi_2) + B\,, \tag{1}$$

where: u_i and φ_i are, respectively, the axial displacement of points along the axis and the rotation of the cross section of the i-th layer (i=1,2); h_i measures the distance between the interface and the axis of the i-th layer; A and B are two coefficients. Different values of the coefficients A and B describe different types of interfacial regime (elastic, hardening, perfectly plastic, softening or detached) within a step-wise linear approximated description of the nonlinear interface behavior.

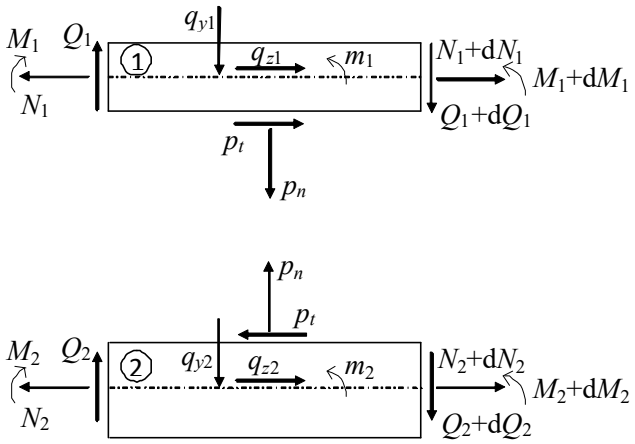

Figure 2. Diagram of the reference structure: distributed loads, internal forces and interfacial tractions for the two-layer beam.

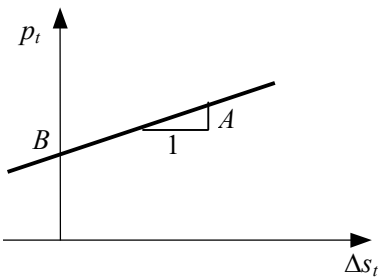

Figure 3. Linear non-proportional interface law.

Rearranging the basic equations described above leads to the following two coupled linear differential equations with constant coefficients for the two unknowns p_t shear and p_n normal tractions at the interface between the layers:

$$\left(K_{\gamma 1}^{-1}+K_{\gamma 2}^{-1}\right)p_n''-\left(K_{\chi 1}^{-1}+K_{\chi 2}^{-1}\right)p_n+\left(K_{\chi 2}^{-1}h_2-K_{\chi 1}^{-1}h_1\right)p_t'=q_n\,, \tag{2a}$$

$$p_t'''-A\left(K_{\varepsilon 1}^{-1}+K_{\varepsilon 2}^{-1}+K_{\chi 1}^{-1}h_1^2+K_{\chi 2}^{-1}h_2^2\right)p_t'+A\left(K_{\chi 2}^{-1}h_2-K_{\chi 1}^{-1}h_1\right)p_n=q_t\,, \tag{2b}$$

having defined

$$q_n=K_{\chi 1}^{-1}\left(q_{y1}+m_1'\right)-K_{\chi 2}^{-1}\left(q_{y2}+m_2'\right)-K_{\gamma 1}^{-1}q_{y1}''-K_{\gamma 2}^{-1}q_{y2}''\,, \tag{3a}$$

$$q_t=A\left[K_{\chi 1}^{-1}h_1\left(q_{y1}+m_1'\right)+K_{\chi 2}^{-1}h_2\left(q_{y2}+m_2'\right)\right]+K_{\varepsilon 1}^{-1}q_{z1}'-K_{\varepsilon 2}^{-1}q_{z2}'\,, \tag{3b}$$

where: primes denote differentiations with respect to z; $K_{\varepsilon i}$, $K_{\gamma i}$ and $K_{\chi i}$ are, respectively, the axial, shear and bending stiffnesses of the i-th layer (i=1,2); q_{zi}, q_{yi} and m_i are continuously varying loads applied to the i-th layer.

The problem admits closed form solution, having general validity independently of the interface regime, for shear and normal interfacial tractions. From the compatibility, equilibrium and constitutive equations for each layer, exact expressions for all other static (namely, N_i, Q_i and M_i respectively axial and shear forces and bending moment in the two layers) and kinematic (namely, u_i, w and φ_i respectively axial displacement, deflection and rotation of the cross section of the two layers) variables of the problem are then derived. The details of the formulation and related solution procedure for uniformly distributed loads are described fully in Campi and Monetto (2013). Such expressions can be extended to the case of continuously varying loads on condition that all terms involving the particular solution of the inhomogeneous differential equations (2) are replaced with analogous ones evaluated for the particular loading distribution prescribed.

It is worth mentioning here that such a fundamental solution of the problem of equilibrium of two-layer beams with interlayer slip contains 17 arbitrary constants to be determined by imposing 17 conditions. The prescription of boundary conditions at the ends gives 5+5=10 conditions to be imposed on w, φ_1, φ_2, u_1, u_2 or, alternatively, on Q=Q_1+Q_2, M_1, M_2, N_1, N_2. Imposing that the displacement discontinuities at the interface between the layers satisfy the bond conditions of perfect connection in the transverse direction and of partial connection in the longitudinal direction for all points of the interface gives 7 additional relations among the arbitrary constants. Such relations depend on both the interface regime and the geometry and material properties of the layers, as detailed in Campi and Monetto (2013) for the special case of composite beams having geometry and material properties satisfying condition (A.1), as in the case of layers having the same geometry and made of the same material.

3. Solution for multi-linear interface laws

Under loading conditions that generate interlayer stresses, interfaces usually exhibit nonlinear behavior corresponding to an irreversible process of progressive debonding. In order to analyze the response of composite beams during such a process, the nonlinear interfacial law can be conveniently approximated through a step-wise linear constitutive equation, as supported by the comparison of experimental and numerical studies (see e.g. Wang, 2007a-b; Planinc et al., 2008). This permits one to employ the fundamental closed form solution presented in Section 2 which is valid for each linear branch.

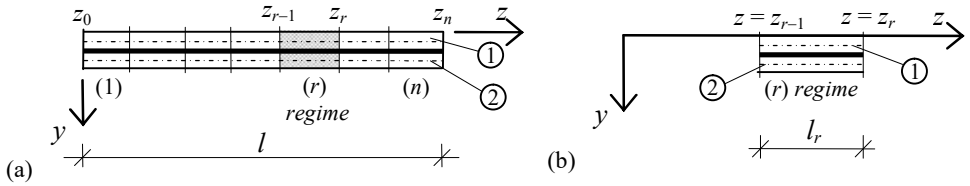

Figure 4. Two-layer composite beam: (a) generic composite beam configuration for multi-linear interface law; (b) generic composite beam element.

In this context, it is reasonable to expect that in a generic configuration the composite beam is divided in n subdomains, as shown in Figure 4a: each composite beam subdomain involves adjacent points along the interface that behave accordingly to the same regime; at the boundaries between two subdomains the limit conditions related to both regimes are valid. The general solution of the equilibrium problem of such a configuration, said physically compatible, consists of n sets of independent functions for normal and shear interfacial stresses, internal forces and displacements: each set refers to a portion of the composite beam. This general solution then totally contains n sets of 17 arbitrary constants. Considering even a low number of regimes coexisting along the interface, the high number of arbitrary constants on which the solution depends suggests a numerical procedure is followed.

In order to do this, it is more convenient to rewrite the proposed solution in vector form (Battini et al., 2009). The basic idea is to express all kinematic and static field variables in vector form as follows:

$$\eta(z) = \mathbf{F}_\eta(z)\mathbf{c} + f_\eta(z) \,, \tag{4}$$

where: η represents any field variable (w, φ_1, φ_2, u_1, u_2 or Q, Q_1, Q_2, M_1, M_2, N_1, N_2, p_t, p_n); $\mathbf{c}$ is the vector 17×1 of the arbitrary constants; $\mathbf{F}_\eta$ is a matrix 1×17 of known functions; f_η is a known scalar function. For prescribed geometry and material properties of the layers, the matrix $\mathbf{F}_\eta$ and the function f_η are derived on the basis of the analytical solution depending on the regime experienced by the interface. Analogously, the additional relations among the arbitrary constants can be written

in vector form as follows:

$$\mathbf{D}\mathbf{c} + \mathbf{d} = \mathbf{0}\,, \tag{5}$$

where $\mathbf{D}$ is a matrix 7×17 and $\mathbf{d}$ is a vector 7×1. As an example, some expressions in vector form are derived in Appendix A for particular geometry and material properties.

The portion of two-layer composite beam, having length l_r, shown in Figure 4b is now considered. All its points along the interface ($z_{r-1} \le z \le z_r$) behave accordingly to the same particular regime, denoted in what follows by superscript "(r)". According to Eq. (4), the vectors $\mathbf{a}_j^{(r)}$ of displacements and $\mathbf{q}_j^{(r)}$ of forces at each end $z=z_j$ ($j=r-1$, r) of the beam element can be written as follows, respectively:

$$\mathbf{a}_j^{(r)} = \begin{Bmatrix} w^{(r)}(z_j) \\ \varphi_1^{(r)}(z_j) \\ \varphi_2^{(r)}(z_j) \\ u_1^{(r)}(z_j) \\ u_2^{(r)}(z_j) \end{Bmatrix} = \begin{bmatrix} \mathbf{F}_w^{(r)}(z_j) \\ \mathbf{F}_{\varphi 1}^{(r)}(z_j) \\ \mathbf{F}_{\varphi 2}^{(r)}(z_j) \\ \mathbf{F}_{u1}^{(r)}(z_j) \\ \mathbf{F}_{u2}^{(r)}(z_j) \end{bmatrix} \mathbf{c}^{(r)} + \begin{Bmatrix} f_w^{(r)}(z_j) \\ f_{\varphi 1}^{(r)}(z_j) \\ f_{\varphi 2}^{(r)}(z_j) \\ f_{u1}^{(r)}(z_j) \\ f_{u2}^{(r)}(z_j) \end{Bmatrix} = \mathbf{X}_j^{(r)}\mathbf{c}^{(r)} + \mathbf{x}_j^{(r)}\,, \tag{6a}$$

$$\mathbf{q}_j^{(r)} = \kappa \begin{Bmatrix} Q^{(r)}(z_j) \\ M_1^{(r)}(z_j) \\ M_2^{(r)}(z_j) \\ N_1^{(r)}(z_j) \\ N_2^{(r)}(z_j) \end{Bmatrix} = \kappa \begin{bmatrix} \mathbf{F}_Q^{(r)}(z_j) \\ \mathbf{F}_{M1}^{(r)}(z_j) \\ \mathbf{F}_{M2}^{(r)}(z_j) \\ \mathbf{F}_{N1}^{(r)}(z_j) \\ \mathbf{F}_{N2}^{(r)}(z_j) \end{bmatrix} \mathbf{c}^{(r)} + \kappa \begin{Bmatrix} f_Q^{(r)}(z_j) \\ f_{M1}^{(r)}(z_j) \\ f_{M2}^{(r)}(z_j) \\ f_{N1}^{(r)}(z_j) \\ f_{N2}^{(r)}(z_j) \end{Bmatrix} = \mathbf{Y}_j^{(r)}\mathbf{c}^{(r)} + \mathbf{y}_j^{(r)}\,, \tag{6b}$$

where: $\mathbf{c}^{(r)}$ is the vector of 17 unknown constants; $\mathbf{X}_j^{(r)}$, $\mathbf{Y}_j^{(r)}$ are known matrices 5×17; $\mathbf{x}_j^{(r)}$, $\mathbf{y}_j^{(r)}$ are known vectors 5×1; $\kappa = 2(j-r)+1$ is introduced to adjust the sign of internal forces to the global coordinate system y, z shown in Figure 4.

As shown in Appendix B, from Eq.s (6) exact stiffness matrix and nodal force vector for a two-layer beam element with interlayer slip to employ in finite element analyses can be derived. In what follows, the attention is focused on the procedure to determine the n sets of unknown constants to employ in semi-analytical solutions.

At each end of the composite beam 5 boundary conditions involving kinematic and/or static quantities depending on the type of constraint can be imposed and expressed in vector form as:

$$\mathbf{B}_j^{(\rho)}\mathbf{c}^{(\varrho)} + \mathbf{b}_j^{(\varrho)} = \bar{\mathbf{b}}_j \quad \text{with } j = 0, n, \tag{7}$$

where: subscript j and superscript $\varrho = \frac{(j+1)(n-j)+jn}{n}$ refer to the ends $z=z_0=0$ ($j=0$, $\rho=1$) or $z=z_n=l$ ($j=n$, $\rho=n$) of the beam and related beam elements; $\mathbf{B}_j^{(\rho)}$ is a known matrix 5×17; $\mathbf{b}_j^{(\varrho)}$, $\bar{\mathbf{b}}_j$ are known vectors 5×1. As an example, Table 1 summarizes some types of end constraint. Furthermore, at each cross-section separating two subdomains 10 continuity conditions on all kinematic and static variables must be imposed and can be expressed in vector form as:

$\mathbf{a}_r^{(r)} = \mathbf{a}_r^{(r+1)}$ and $\mathbf{q}_r^{(r)} = \mathbf{q}_r^{(r+1)}$ with r =1,..., n–1. (8)

In addition, for each subdomain 7 additional relations among unknown constants must be satisfied:

$\mathbf{D}^{(r)}\mathbf{c}^{(r)} + \mathbf{d}^{(r)} = \mathbf{0}$ with r =1,..., n. (9)

In conclusion, Eq.s (7)-(9) are 17×n algebraic equations for the n sets of 17 unknown constants contained in the general solution of the problem of equilibrium of the two-layer composite beam with interlayer slip in a generic configuration.

	Fixed end w=u_1=u_2=0 φ_1=φ_2=0	Loaded end κQ=P N_1=N_2=0 M_1=M_2=0	Supported end w=u_2=0 N_1=0 M_1=M_2=0
$\mathbf{B}_j^{(\varrho)}$	$\mathbf{X}_j^{(\varrho)}$	$\mathbf{Y}_j^{(\varrho)}$	$[\mathbf{F}_w^{(\varrho)}(z_j)\ \kappa\mathbf{F}_{M1}^{(\varrho)}(z_j)\ \kappa\mathbf{F}_{M2}^{(\varrho)}(z_j)\ \kappa\mathbf{F}_{N1}^{(\varrho)}(z_j)\ \mathbf{F}_{u2}^{(\varrho)}(z_j)]^{\mathrm{T}}$
$\mathbf{b}_j^{(\varrho)}$	$\mathbf{x}_j^{(\varrho)}$	$\mathbf{y}_j^{(\varrho)}$	$\{f_w^{(\varrho)}(z_j)\ \kappa f_{M1}^{(\varrho)}(z_j)\ \kappa f_{M2}^{(\varrho)}(z_j)\ \kappa f_{N1}^{(\varrho)}(z_j)\ f_{u2}^{(\varrho)}(z_j)\}^{\mathrm{T}}$
$\bar{\mathbf{b}}_j$	**0**	{P 0 0 0 0}$^{\mathrm{T}}$	**0**

Table 1. Boundary conditions for some types of end constraint, being $\kappa = [(j+1)(j-n)+j]/n$ (j=0, n).

Firstly, the combination of Eq.s (8) with Eq.s (6) and Eq.s (9) leads to n–1 systems of 17 algebraic equations:

$$\begin{Bmatrix}\mathbf{a}_r^{(r)}\\ \mathbf{q}_r^{(r)}\\ \mathbf{0}_7\end{Bmatrix} = \begin{bmatrix}\mathbf{X}_r^{(r)}\\ \mathbf{Y}_r^{(r)}\\ \mathbf{D}^{(r)}\end{bmatrix}\mathbf{c}^{(r)} + \begin{Bmatrix}\mathbf{x}_r^{(r)}\\ \mathbf{y}_r^{(r)}\\ \mathbf{d}^{(r)}\end{Bmatrix} = \begin{Bmatrix}\mathbf{a}_r^{(r+1)}\\ \mathbf{q}_r^{(r+1)}\\ \mathbf{0}_7\end{Bmatrix} = \begin{bmatrix}\mathbf{X}_r^{(r+1)}\\ \mathbf{Y}_r^{(r+1)}\\ \mathbf{D}^{(r+1)}\end{bmatrix}\mathbf{c}^{(r+1)} + \begin{Bmatrix}\mathbf{x}_r^{(r+1)}\\ \mathbf{y}_r^{(r+1)}\\ \mathbf{d}^{(r+1)}\end{Bmatrix} \quad \text{with } r=1,\ldots,n-1, \tag{10}$$

from which the vector of unknown constants related to each beam element can be expressed in terms of that related to the next beam element:

$$\mathbf{c}^{(r)} = \begin{bmatrix}\mathbf{X}_r^{(r)}\\ \mathbf{Y}_r^{(r)}\\ \mathbf{D}^{(r)}\end{bmatrix}^{-1}\begin{bmatrix}\mathbf{X}_r^{(r+1)}\\ \mathbf{Y}_r^{(r+1)}\\ \mathbf{D}^{(r+1)}\end{bmatrix}\mathbf{c}^{(r+1)} + \begin{bmatrix}\mathbf{X}_r^{(r)}\\ \mathbf{Y}_r^{(r)}\\ \mathbf{D}^{(r)}\end{bmatrix}^{-1}\begin{Bmatrix}\mathbf{x}_r^{(r+1)}-\mathbf{x}_r^{(r)}\\ \mathbf{y}_r^{(r+1)}-\mathbf{y}_r^{(r)}\\ \mathbf{d}^{(r+1)}-\mathbf{d}^{(r)}\end{Bmatrix} = \mathbf{Z}^{(r+1)}\mathbf{c}^{(r+1)} + \mathbf{z}^{(r+1)} \quad \text{with } r=1,\ldots,n-1 \tag{11}$$

and $\mathbf{Z}^{(r+1)}$, $\mathbf{z}^{(r+1)}$ being a square matrix 17×17 and a vector 17×1, respectively. Proceeding in the same manner over the n layers, the unknown constants related to the first beam element can then be expressed in terms of those related to the last beam element:

$$\mathbf{c}^{(1)} = \left(\prod_{k=2}^{n}\mathbf{Z}^{(k)}\right)\mathbf{c}^{(n)} + \left[\sum_{m=3}^{n}\left(\prod_{k=2}^{m-1}\mathbf{Z}^{(k)}\right)\mathbf{z}^{(m)}\right] + \mathbf{z}^{(2)} = \hat{\mathbf{Z}}\mathbf{c}^{(n)} + \hat{\mathbf{z}}\,, \tag{12}$$

where $\hat{\mathbf{Z}}$ is a square matrix 17×17 and $\hat{\mathbf{z}}$ is a vector 17×1.

Secondly, substituting Eq. (12) in Eq. (7) for j=0 and combining the result with Eq. (7) for j=n and with Eq. (9) having set r=n gives a system of 17 algebraic equations for the unknown constants related to the last beam portion:

$$\begin{bmatrix}\mathbf{B}_0^{(1)}\mathbf{c}^{(1)} + \mathbf{b}_0^{(1)} - \bar{\mathbf{b}}_0\\ \mathbf{B}_n^{(n)}\mathbf{c}^{(n)} + \mathbf{b}_n^{(n)} - \bar{\mathbf{b}}_n\\ \mathbf{D}^{(n)}\mathbf{c}^{(n)} + \mathbf{d}^{(n)}\end{bmatrix} = \begin{bmatrix}\mathbf{B}_0^{(1)}\hat{\mathbf{Z}}\\ \mathbf{B}_n^{(n)}\\ \mathbf{D}^{(n)}\end{bmatrix}\mathbf{c}^{(n)} + \begin{Bmatrix}\mathbf{B}_0^{(1)}\hat{\mathbf{z}} + \mathbf{b}_0^{(1)} - \bar{\mathbf{b}}_0\\ \mathbf{b}_n^{(n)} - \bar{\mathbf{b}}_n\\ \mathbf{d}^{(n)}\end{Bmatrix} = \mathbf{W}\mathbf{c}^{(n)} + \mathbf{w} = \mathbf{0}\,, \tag{13}$$

where $\mathbf{W}$ is a square matrix 17×17 and $\mathbf{w}$ is a vector 17×1. From Eq. (13) we finally obtain the n-th set of arbitrary constants:

$$\mathbf{c}^{(n)} = -\mathbf{W}^{-1}\mathbf{w} \,. \tag{14}$$

Finally, the other $n-1$ sets of arbitrary constants are determined by combining Eq.s (14) and (11) over the remaining beam subdomains. This completes the general solution of the problem of equilibrium of two-layer beams with interlayer slip and multi-linear interface law in a generic configuration.

The formulation detailed above with reference to simple straight beams constrained at the opposite ends can be extended to more complicated beam structures. As an example, at each cross section where two beams are joined by hinges, such as in the case of Gerber beams, the continuity conditions (8) related to layer rotations must be replaced by conditions of nil moments in the two layers. Furthermore, at each cross section at which continuous beams rest on interior supports an additional condition of nil deflection must be added to boundary conditions (7). Analogously, at each cross section where point forces are applied the continuity conditions (8) related to axial or shear forces in the layers must be suitably modified to take into account the presence of external forces. Finally, in the more complicated case of frames, continuity conditions (8) and additional relations (9) for each simple beam composing the frame must be firstly written with reference to local coordinates and then transformed in global coordinates through suitable rotation matrices.

It is worth noting that the length of each beam subdomain is unknown a priori, since interface regimes depend on the load level. The simulation of a process of progressive interface debonding in composite beams under loading conditions that generate interlayer stresses is then a nonlinear problem which can be solved by analyzing a sequence of consecutive physically compatible configurations and evaluating the load levels for which such configurations are also equilibrated. Depending on the complexity of such configurations incremental or incremental-iterative procedures must be followed. Such a complexity correlates with the number of subdomains, that is of simultaneous regimes experienced along the interface, and depends not only on the type of step-wise interface law but also on the type of beam structure, that is on geometry as well as on loading and constraining conditions. It follows that a unified numerical procedure cannot be defined.

4. Numerical examples

In this section, two sets of numerical results are shown. Firstly, in order to validate the employment of the fundamental closed form solution to practical applications, a comparison with results found in literature is presented. Secondly, the response of two-layer beams with partial composite action during a loading process inducing a progressive debonding of the interface is

simulated and the influence of interface parameters on the stiffness and collapse load of the composite structural elements is discussed.

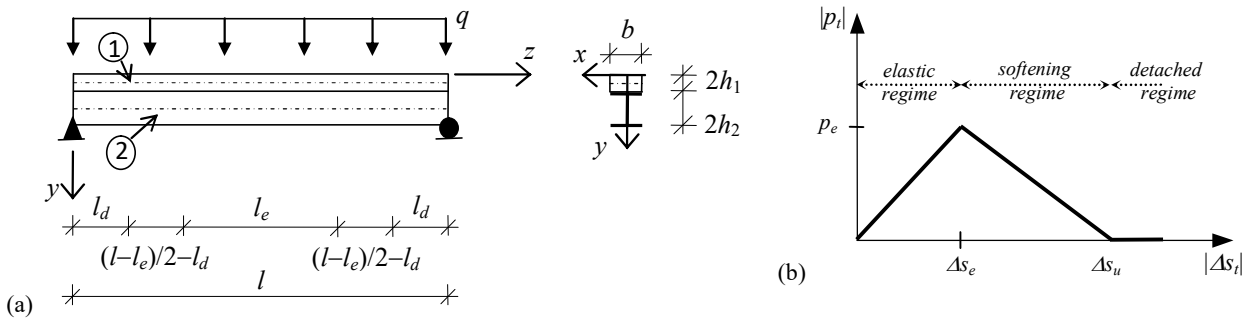

Figure 5. Two-layer simply supported RC-steel composite beam (Foraboschi, 2009): (a) geometry; (b) interface law.

The first numerical example refers to a simply supported beam composed of reinforced concrete (RC) and steel and subjected to uniformly distributed transverse load, as shown in Figure 5a. The elastic-damaging three-linear interface law shown in Figure 5b is assumed to describe the imperfect connection between concrete and steel in the longitudinal direction: the interface exhibits firstly an elastic behavior ($A=p_e/\Delta s_e>0$, $B=0$) until the elastic limit is reached ($|p_t|=p_e$), then a softening regime ($A=p_e/(\Delta s_e-\Delta s_u)<0$, $B=p_e\Delta s_u/(\Delta s_u-\Delta s_e)$), until debonding initiates ($|\Delta s_t|=\Delta s_u$), and finally a detached regime ($A=B=0$), which characterizes the incapacity of interface of transmitting any shear traction as if the beam consists of two separate layers. For this example the input data are the geometry and material properties of the layers and the parameters characterizing the interface law (the initial elastic stiffness, the elastic limit shear traction and the ultimate slip, from which coefficients A and B for each linear branch of the interface law can be calculated), summarized in the first two columns of Table 2. The output is the beam configuration equilibrated with a specific load level considered previously by Foraboschi (2009). As shown in Figure 5a, because of the high load level, the interface is assumed to be divided in five portions: one central portion, having length l_e, which undergoes the elastic regime; two lateral portions, having each length l_d, positioned adjacent to the ends and symmetrically with respect to midspan, which undergo the detached regime; two intermediate portions, which undergo the softening regime. The problem is nonlinear since the lengths l_e and l_d depend on the load level and are unknown a priori. In order to find a solution, they are assumed as non conventional parameters to control the debonding process. In particular, the length of the elastic portion of the interface is decreased monotonically and for each value the length of the detached portion is iteratively increased until an equilibrated configuration is found and the related load level is calculated. The incremental-iterative procedure is arrested at the specific load level under consideration. In the third column of Table 2 some significant numerical results obtained with the approach presented are compared with those found previously by

Foraboschi (2009): namely, the length of the elastic and detached portions of the interface, maximum slip and shear traction at one supported end and axial forces in each layer at midspan for the particular load level under consideration. A good agreement between the two sets of results in terms of percentage relative error (less than 7% in absolute value) is observed. The same example was considered by Focacci et al. (2015) to compare their results and show the accuracy of their solution.

Geometry and material properties	Interface stiffness and model parameters	Numerical results			
			Foraboschi (2009)	present model	relative error [%]
l = 820 cm	p_e = 2.25 kN/cm				
b = 30 cm	Δs_e = 0.65 mm				
$2h_1$ = 5 cm	Δs_u = 1.12 mm	q [kN/m]	57.25	57.31	0.11
$2h_2$ = 29 cm	elastic regime:	l_e [cm]	594	618	4.04
$K_{\varepsilon 1}$ = 375 MN	A = 346 MPa	l_d [cm]	0	0	-
$K_{\chi 1}$ = 781.25 MN cm^2	softening regime:	Δs_t [mm] at z = 0	0.826	0.833	0.85
$K_{\varepsilon 2}$ = 2373 MN	A = –479 MPa	p_t [kN/cm] at z = 0	1.47	1.37	–6.80
$K_{\chi 2}$ = 383460 MN cm^2	B = 5.36 kN/cm	N_1=– N_2 [kN] at z = l/2	–530	–500	–5.84

Table 2. Model parameters and significant results for RC-steel composite beam.

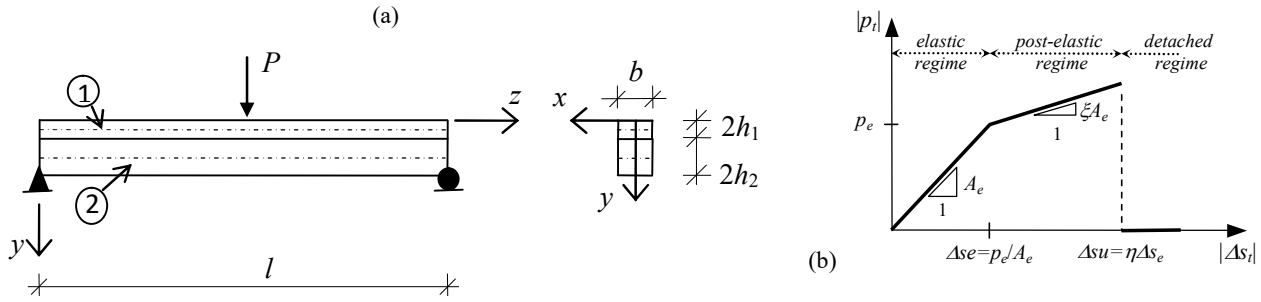

Figure 6. Two-layer wood composite beam: (a) geometry; (b) interface law.

Secondly, a simply supported two-layer wood composite beam under point load at midspan is considered. With reference to Figure 6a, the two layers have constant rectangular cross sections of identical width but different heights (l=300cm, b=12cm, $2h_1$=5cm, $2h_2$=14cm) and are made of the same linearly elastic and homogeneous material (Young modulus E=11500MN). The nonlinear behavior of the imperfect connection in the longitudinal direction is described by the three-linear interface law shown in Figure 6b. Such interfacial model differs from that shown in Figure 5b in the post-elastic regime ($A=\xi A_e$, $B=p_e(1-\xi)$) experienced by the interface after the elastic limit is reached until debonding initiates. Depending on the value prescribed for ξ, different post-elastic regimes can be considered and different types of joints can be modelled: $0<\xi<1$ or $\xi=0$ corresponds to a hardening or plastic regime, which suitably describes joints realized through mechanical shear devices, such as nails and steel studs; $\xi<0$ corresponds to a softening regime, which suitably describes sufficiently thin adhesive joints. Four parameters characterize this model: the initial

elastic stiffness A_e, the elastic limit shear traction p_e, the ratio ξ of post-elastic to elastic stiffness and the ratio η of ultimate to elastic limit slip.

For this example the input data are the geometry and material properties of the layers and the parameters characterizing the interface law, which are varied in order to analyze the influence of the post-elastic interface behavior on the debonding process. The output is the sequence of consecutive equilibrated beam configurations and related load levels and static and kinematic field variables.

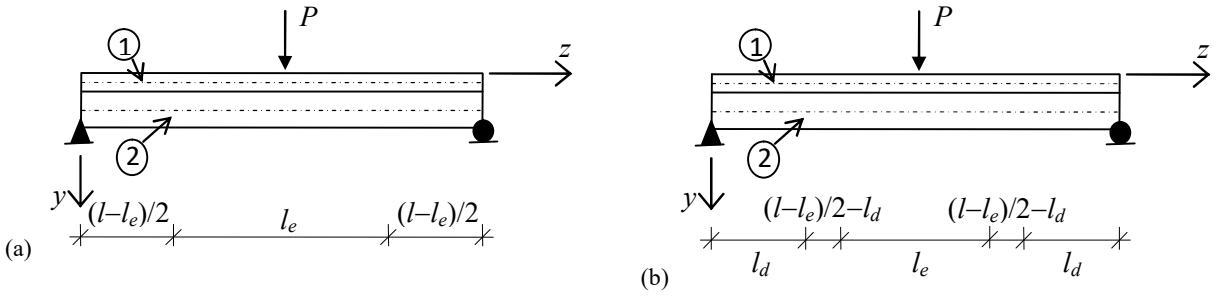

Figure 7. Two-layer wood composite beam: generic post-elastic configurations.

As well known, shear traction and slip have maximum absolute values at the ends of the beam (z=0 and z=l) where first the elastic limit is reached and then debonding initiates. Such an irreversible process involves adjacent points and proceeds along the interface towards midspan ($z = l/2$). Analogously to the previous example, the generic configuration of the beam then changes from the one characterized by the whole interface undergoing the elastic behavior first to the one shown in Figure 7a and then to the one shown in Figure 7b. The configuration shown in Figure 7a differs from the one shown in Figure 7b in the absence of the interface portion debonded (l_d=0). Because of the irreversibility of such a progressive damage and debonding process, l_e decreases monotonically whereas l_d increases monotonically; they can so be assumed as non conventional parameters to control the process in order to catch any branch of the load – midspan deflection curve (including possible snap-through or snap-back branches).

In particular, firstly, with reference to the post-elastic configuration shown in Figure 7a, starting from the initial value l_e=l, l_e is decreased incrementally and monotonically. For each prescribed value for l_e, the load level for which the related configuration is not only equilibrated (i.e. satisfying the general solution described in Section 3) but also physically compatible (i.e. $|p_t|$=p_e at the boundaries between the elastic and post-elastic portions and $|\Delta_{st}|<\Delta_{su}$ at the ends) is calculated. The incremental procedure is arrested as soon as $|\Delta_{st}|\geq\Delta_{su}$ at the ends of the beam, since this denotes that interface debonding initiates and a change of configuration occurs. Secondly, with reference to the most generic configuration shown in Figure 7b, once again l_e is decreased incrementally and monotonically. For each prescribed value for l_e, l_d is iteratively increased until a configuration both equilibrated and physically compatible (i.e. $|p_t|$=p_e at the boundaries between the elastic and post-

elastic portions and $|\Delta_{sl}|=\Delta_{su}$ at the boundaries between the post-elastic and debonded portions) is found and the related load level is calculated.

The mechanical responses of composite beams so simulated are summarized through load – midspan deflection curves, as shown by dimensionless diagrams in Figures 8 to 11. It is straightforward that such responses are affected by geometry and material properties of both layers and interface. As an example, the first linear branch describes the initial elastic response of the system; the related global stiffness, defined as the ratio of applied load to midspan deflection (say $w_{\max}$), and elastic strength, defined as the maximum load carried until interface undergoes only elastic deformation, depend on A_e and p_e, respectively: the higher A_e, the higher the initial global stiffness of the composite beam; the higher p_e, the higher the elastic strength. In this paper the attention is focused on the influence of the post-elastic interfacial behavior on the response of the composite beam. In order to investigate this, a parametric analysis is performed by varying the value of interface parameters related to post-elastic and detached regimes. Figures 8 to 11 show the results obtained for $A_e = 100$ MPa, $p_e = 50$ kN/m and different values of $\xi = 0.5, 0, -0.5, -2$ and $\eta = 1.5, 3$. These results permit several interesting conclusions.

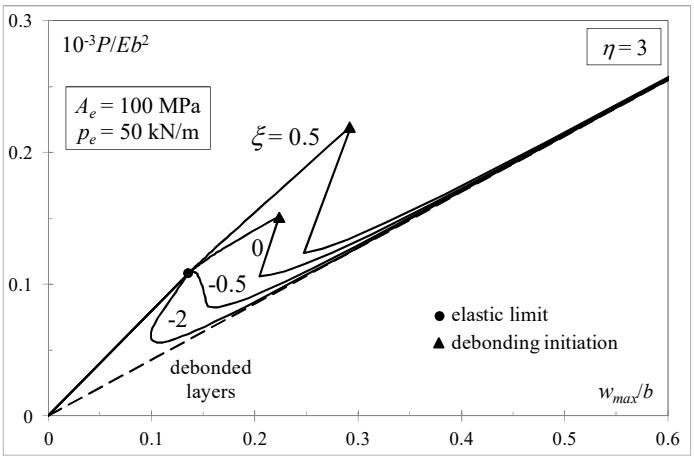

Figure 8. Two-layer wood composite beam: load – midspan deflection curves for varying ratio of the post-elastic to the elastic interfacial stiffness.

Figure 8 shows the response of the simply supported two-layer beam for different post-elastic interfacial regimes. All responses have the same initial linear elastic branch but then differ in the nonlinear branch depending on the value of paramaeter ξ. Beams with either hardening ($\xi>0$) or plastic ($\xi=0$) interface undergo a reduction in the global stiffness but their strength results to be increased significantly with respect to the elastic limit. Namely, the strength of the composite beam is here defined as the maximum load carried until interface debonding initiates. For all beams, finally, debonding initiation is followed by a prominent snap-back branch, catched because of the non conventional choice of control parameters discussed above; then, the response tends to that of the beam with the interface completely debonded (dashed line).

Figures 9 to 11 show the effects of the variation of the utimate slip of the interface, as a measure of interface ductility, on the strength of the simply supported two-layer beam.

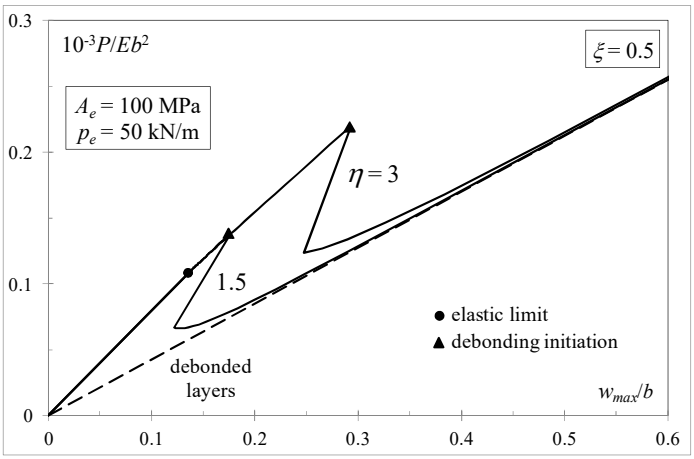

Figure 9. Two-layer wood composite beam: load – midspan deflection curves for hardening interface with varying ratio of the utimate to the elastic limit interfacial slip.

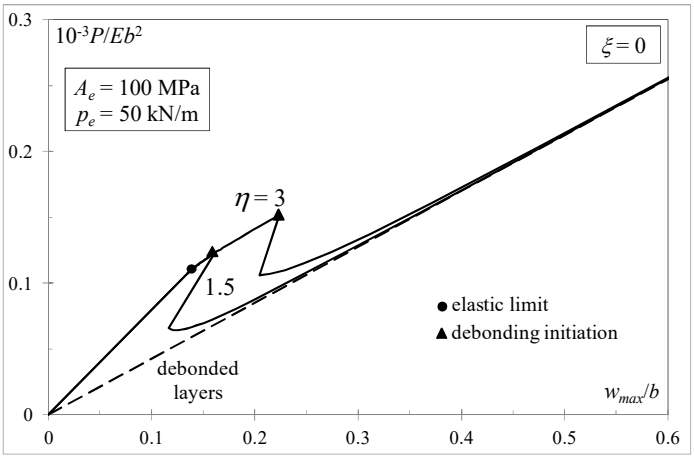

Figure 10. Two-layer wood composite beam: load – midspan deflection curves for plastic interface with varying ratio of the utimate to the elastic limit interfacial slip.

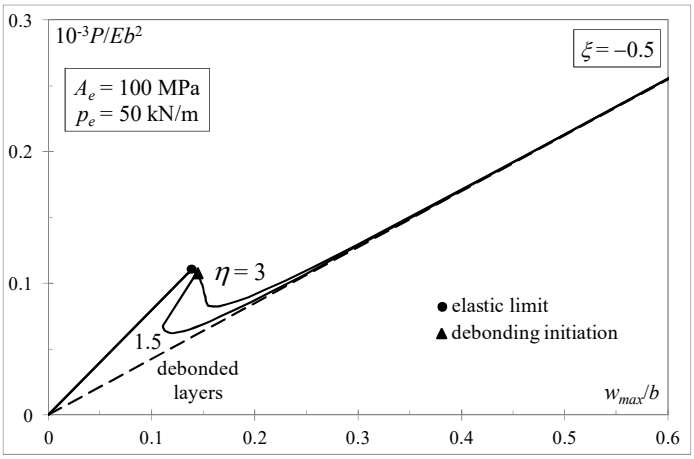

Figure 11. Two-layer wood composite beam: load – midspan deflection curves for softening interface with varying ratio of the utimate to the elastic limit interfacial slip.

With reference to Figures 9 and 10, on increasing η, an increase in the strength is produced. This increase is more important for beams with hardening (ξ>0) than plastic (ξ=0) interface. For η=1.5, the maximum load ranges from 115% for ξ=0 to 129% for ξ=0.5 of the elastic strength. For η=3, the maximum load ranges from less than 1.5 times for ξ=0 to more than 2 times for ξ=0.5 the elastic strength. On the contrary, no significant effects are detected for beams with softening interface (ξ<0), as shown in Figure 11.

5. Conclusions

The nonlinear problem of two-layer beams with interlayer slip and nonlinear interface law under loading conditions that induce an irreversible process of progressive debonding at the interface is analyzed by solving the equilibrium problem of a sequence of consecutive beam configurations obtained by progressively decreasing the length of the interface portion experiencing an elastic behavior and increasing the length of portions experiencing post-elastic regimes. In particular, the attention is focused on nonlinear interfacial behaviors which can be suitably approximated through step-wise linear laws. This permits one to employ the fundamental analytical solution derived by the authors in a previous paper with reference to a linear non-proportional interface law able to describe different types of interfacial regimes (elastic, hardening, perfectly-plastic, softening or detached) depending on the value of some model parameters. Such a fundamental solution is employed to solve the equilibrium problem for each configuration and to evaluate the related load level by imposing the conditions of physical compatibility at the boundaries between two beam portions experiencing different interfacial regimes.

Compared to a previous work by the authors (Campi and Monetto, 2013), this paper deals with a vector form of the solution of the equilibrium problem for a generic beam configuration. From one hand, as main goal of the present paper, this facilitates the determination of the arbitrary constants to employ in a semi-analytical procedure for simulating the interface debonding. On the other, the derivation of exact stiffness matrix and end force vector for a composite beam element to employ in finite element analyses, avoiding curvature locking problems, is allowed.

The numerical results obtained show the validity and applicability of the semi-analytical procedure proposed as an alternative method of solution or as a method of validation for finite element analyses.

To conclude, it is worth noting that the formulation could be extended to an even wider class of nonlinear problems (e.g. step-wise linear interface laws characterized by an unlimited number of linear branches, continuous beams or frames, layers behaving anelastically according to step-wise linear constitutive law) than those considered here but at the expense of a much more complicated incremental-iterative solution procedure which is not of interest to this paper.

Acknowledgements

Support from the University of Genoa and the Italian Ministry of Instruction, University and Research (MIUR), within the Joint Research Projects on "Multiscale mechanical interactions in multilayered materials" and "Multi-scale modelling of materials and structures" (MIUR PRIN09 n. 2009XWLFKW), is gratefully acknowledged.

Appendix A. Exemple of expressions in vector form

This Appendix details the procedure for rewriting in vector form the exact expressions for all kinematic and static field variables found by Campi and Monetto (2013). As an example, interfacial normal tractions and additional relations among the arbitrary constants are considered. In particular, the attention is focused on the special case of composite beams consisting of two layers having geometry and material properties satisfying the condition:

$$K_{\chi 2}^{-1} h_2 - K_{\chi 1}^{-1} h_1 = 0 \,. \tag{A1}$$

For the case under consideration, Campi and Monetto (2013) showed that the general solution of Eq.s (2) for interfacial normal tractions p_n results:

$$p_n(z) = c_1 \cosh(\alpha\, z) + c_2 \sinh(\alpha\, z) + \bar{p}_n \,, \tag{A2}$$

where:

$$\alpha = \sqrt{\left(K_{\gamma 1}^{-1} + K_{\gamma 2}^{-1}\right)^{-1} \left(K_{\chi 1}^{-1} + K_{\chi 2}^{-1}\right)} \,, \tag{A3}$$

whereas c_1 and c_2 are the first two arbitrary constants and $\bar{p}_n$ is the particular solution depending on the distribution of the external loads which, as an example, for uniformly distributed loads yields:

$$\bar{p}_n = \left(K_{\chi 1}^{-1} + K_{\chi 2}^{-1}\right)\left(K_{\chi 2}^{-1} q_{y2} - K_{\chi 1}^{-1} q_{y1}\right) \,. \tag{A4}$$

It is straightforward that Eq. (A2) can be written alternatively as:

$$p_n(z) = [\cosh(\alpha\, z) \quad \sinh(\alpha\, z) \quad \mathbf{0}_{15}^{\mathrm{T}}]\, \mathbf{c} + \bar{p}_n \,, \tag{A5}$$

from which, accordingly to Eq. (4), it follows:

$$\mathbf{F}_{pn}(z) = [\cosh(\alpha\, z) \quad \sinh(\alpha\, z) \quad \mathbf{0}_{15}^{\mathrm{T}}] \quad \text{and} \quad f_\eta(z) = \bar{p}_n \,, \tag{A6}$$

where $\mathbf{0}_{15}$ is the zero vector having 15 components.

Analogously, Campi and Monetto (2013) found the following additional relations among the arbitrary constants for an interface law with A=0:

$$\begin{cases} K_{\chi 2}^{-1}(m_2 - c_9) - K_{\chi 1}^{-1}(m_1 - c_8) = 0 \\ K_{\gamma 2}^{-1} c_9 - K_{\gamma 1}^{-1} c_8 + c_{14} - c_{15} = 0 \\ c_{16} - c_{17} = 0 \\ \left(K_{\chi 1}^{-1} + K_{\chi 2}^{-1}\right)^{-1} (K_{\gamma 1}^{-1} K_{\chi 2}^{-1} - K_{\gamma 2}^{-1} K_{\chi 1}^{-1})(q_{y1} + q_{y2}) + K_{\chi 1}^{-1} c_{10} - K_{\chi 2}^{-1} c_{11} = 0 \\ c_3 = 0 \\ c_4 = 0 \\ c_5 = B \end{cases} . \tag{A7}$$

Taking into account Eq. (5), it is straightforward that the non-zero components of the matrix **D** and vector **d** are:

$$\begin{aligned} &D_{1,8} = D_{4,10} = K_{\chi 1}^{-1}, \quad D_{2,8} = -K_{\gamma 1}^{-1}, \quad D_{2,14} = D_{3,16} = D_{5,3} = D_{6,4} = D_{7,5} = 1, \\ &D_{1,9} = D_{4,11} = -K_{\chi 2}^{-1}, \quad D_{2,9} = K_{\gamma 2}^{-1}, \quad D_{2,15} = D_{3,17} = -1, \end{aligned} \tag{A8a}$$

and:

$$d_1 = K_{\chi 2}^{-1} m_2 - K_{\chi 1}^{-1} m_1, \quad d_4 = \left(K_{\chi 1}^{-1} + K_{\chi 2}^{-1}\right)^{-1} \left(K_{\gamma 1}^{-1} K_{\chi 2}^{-1} - K_{\gamma 2}^{-1} K_{\chi 1}^{-1}\right)\left(q_{y1} + q_{y2}\right), \quad d_7 = -B. \tag{A8b}$$

Appendix B. Exact stiffness matrix and end force vector for a composite beam element

As shown in this Appendix, the vector form of the fundamental closed form solution considered in Section 3 can be employed also to derive the exact stiffness matrix and nodal force vector for a two-layer beam element with interlayer slip to employ in finite element analyses.

In order to do this, the generic element of two-layer composite beam, having length l_r, shown in Figure 4b is considered. From Eq.s (6) the vectors of end displacements, say $\hat{\mathbf{a}}^{(r)}$, and forces, say $\hat{\mathbf{q}}^{(r)}$, for the beam element result:

$$\hat{\mathbf{a}}^{(r)} = \begin{Bmatrix} \mathbf{a}_{r-1}^{(r)} \\ \mathbf{a}_{r}^{(r)} \end{Bmatrix} = \begin{bmatrix} \mathbf{X}_{r-1}^{(r)} \\ \mathbf{X}_{r}^{(r)} \end{bmatrix} \mathbf{c}^{(r)} + \begin{Bmatrix} \mathbf{x}_{r-1}^{(r)} \\ \mathbf{x}_{r}^{(r)} \end{Bmatrix} = \hat{\mathbf{X}}^{(r)} \mathbf{c}^{(r)} + \hat{\mathbf{x}}^{(r)}, \tag{B1a}$$

$$\hat{\mathbf{q}}^{(r)} = \begin{Bmatrix} \mathbf{q}_{r-1}^{(r)} \\ \mathbf{q}_{r}^{(r)} \end{Bmatrix} = \begin{bmatrix} \mathbf{Y}_{r-1}^{(r)} \\ \mathbf{Y}_{r}^{(r)} \end{bmatrix} \mathbf{c}^{(r)} + \begin{Bmatrix} \mathbf{y}_{r-1}^{(r)} \\ \mathbf{y}_{r}^{(r)} \end{Bmatrix} = \hat{\mathbf{Y}}^{(r)} \mathbf{c}^{(r)} + \hat{\mathbf{y}}^{(r)}, \tag{B1b}$$

where $\hat{\mathbf{X}}^{(r)}$, $\hat{\mathbf{Y}}^{(r)}$ are matrices 10×17 and $\hat{\mathbf{x}}^{(r)}$, $\hat{\mathbf{y}}^{(r)}$ are vectors 10×1. Combining Eq. (B1a) with the additional relations among the arbitrary constants, given by Eq. (5) in general terms, leads to the following system of 17 algebraic equations:

$$\tilde{\mathbf{a}}^{(r)} = \begin{Bmatrix} \hat{\mathbf{a}}^{(r)} \\ \mathbf{0}_7 \end{Bmatrix} = \begin{bmatrix} \hat{\mathbf{X}}^{(r)} \\ \mathbf{D}^{(r)} \end{bmatrix} \mathbf{c}^{(r)} + \begin{Bmatrix} \hat{\mathbf{x}}^{(r)} \\ \mathbf{d}^{(r)} \end{Bmatrix} = \tilde{\mathbf{X}}^{(r)} \mathbf{c}^{(r)} + \tilde{\mathbf{x}}^{(r)}, \tag{B2}$$

where $\tilde{\mathbf{a}}^{(r)}$, $\tilde{\mathbf{x}}^{(r)}$ are vectors 17×1 and $\tilde{\mathbf{X}}^{(r)}$ is a square matrix 17×17, whereas $\mathbf{0}_7$ is the zero vector having 7 components. Following the direct stiffness approach (Battini et al., 2009), from Eq. (B2) the vector of unknown constants can be expressed in terms of end displacements:

$$\mathbf{c}^{(r)} = \tilde{\mathbf{X}}^{(r)^{-1}} \left(\tilde{\mathbf{a}}^{(r)} - \tilde{\mathbf{x}}^{(r)}\right). \tag{B3}$$

Substituting Eq. (B3) into Eq. (B1b) finally gives also end forces in terms of end displacements:

$$\hat{\mathbf{q}}^{(r)} = \left(\hat{\mathbf{Y}}^{(r)} \tilde{\mathbf{X}}^{(r)^{-1}}\right) \tilde{\mathbf{a}}^{(r)} + \left(\hat{\mathbf{y}}^{(r)} - \hat{\mathbf{Y}}^{(r)} \tilde{\mathbf{X}}^{(r)^{-1}} \tilde{\mathbf{x}}^{(r)}\right) = \tilde{\mathbf{K}}^{(r)} \tilde{\mathbf{a}}^{(r)} + \hat{\mathbf{q}}_0^{(r)} = \hat{\mathbf{K}}^{(r)} \hat{\mathbf{a}}^{(r)} + \hat{\mathbf{q}}_0^{(r)}, \tag{B4}$$

where: $\tilde{\mathbf{K}}^{(r)}$ is a matrix 10×17, whereas $\hat{\mathbf{K}}^{(r)}$ is a matrix 10×10 obtained by deleting the last 7 columns of $\tilde{\mathbf{K}}^{(r)}$; $\hat{\mathbf{q}}_0^{(r)}$ is a vector 10×1. In particular, $\hat{\mathbf{K}}^{(r)}$ and $\hat{\mathbf{q}}_0^{(r)}$ defined by Eq. (B4) represent, respectively, the exact stiffness matrix and nodal force vector for the beam finite element under consideration.

It is worthwhile noting that, since the stiffness matrix and nodal force vector given by Eq. (B4) derive from the exact solution of the equilibrium problem of two-layer beams with interlayer slip, their employment in finite element analyses allows to avoid curvature locking generally encountered with low order polynomial finite elements (see e.g. Ranzi, 2008).

References

Baraldi D., Cecchi A., Foraboschi P., 2016. Broken tempered laminated glass: Non-linear discrete element modeling. Composite Structures 140, 278-295.

Battini, J.M., Nguyen, Q.H., Hjiaj, M., 2009. Non-linear finite element analysis of composite beams with interlayer slips. Comput. Struct. 87, 904-912.

Bennati, S., Colleluori, M., Corigliano, D., Valvo, P.S., 2009. An enhanced beam-theory model of the asymmetric double cantilever beam (ADCB) test for composite laminates. Compos. Science Tech. 69, 1735-1745.

Campi, F., Monetto, I., 2013. Analytical solutions of two-layer beams with interlayer slip and bi-linear interface law. Int. J. Solids Structures 50, 687-698.

Čas B., Bratina S., Saje M., Planinc I., 2004. Non-linear analysis of composite steel-concrete beams with incomplete interaction. Steel and Composite Structures 4, 489-507.

Cosenza, E., Mazzolani, S., 1993. Analisi in campo lineare di travi composte con connessioni deformabili: formule esatte e risoluzione alle differenze finite. Proc. First Italian Workshop on Composite structures, University of Trento, 1-21 (in Italian).

Focacci F., Foraboschi P., De Stefano M., 2015. Composite beam generally connected: Analytical model. Composite Structures 133, 1237-1248.

Foraboschi, P., 2009. Analytical solution of two-layer beam taking into account nonlinear interlayer slip. J. Eng. Mech. 135, 1129-1146.

Girhammar, U.A., Gopu, V.K.A., 1993. Composite beam-columns with interlayer slip – Exact analysis. J. Struct. Eng. 119, 1265-1282.

Girhammar, U.A., Pan, D.H., 2007. Exact static analysis of partially composite beams and beam-columns. Int. J. Mech. Sciences 49, 239-255.

Hozjan, T., Saje, M., Srpčič, S., Planinc, I., 2013. Geometrically and materially non-linear analysis of planar composite structures with an interlayer slip. Computers and Structures 114-115, 1-17.

Lu, X.Z., Teng, J.G., Ye, L.P., Jiang, J.J., 2005. Bond–slip models for FRP sheets/plates bonded to concrete. Eng. Struct. 27, 920-937.

Newmark, N.M., Siess, C.P., Viest, I.M., 1951. Tests and analysis of composite beams with incomplete interaction. Proc. Society for Experimental Stress Analysis 9, 75-92.

Planinc, I., Schnabl, S., Saje, M., Lopatič, J., Čas, B., 2008. Numerical and experimental analysis of timber composite beams with interlayer slip. Eng. Structures 30, 2959-2969.

Ranzi, G., 2008. Locking problems in the partial interaction analysis of multi-layered composite beams. Eng. Structures 30, 2900-2911.

Schnabl, S., Saje, M., Turk, G., Planinc, I., 2007. Analytical solution of two-layer beam taking into account interlayer slip and shear deformation. J. Struct. Eng. 133, 886-894.

Schreyer, H.L., Peffer, A., 2000. Fiber pullout based on a one-dimensional model of decohesion. Mech. Materials 32, 821-836.

Qiao, P., Wang, J., 2005. Novel joint deformation models and their application to delamination fracture analysis. Compos. Science Tech. 65, 1826-1839.

Wang, J., 2006. Debonding of FRP-plated reinforced concrete beam, a bond-slip analysis. I. Theoretical formulation. Int. J. Solids Struct. 43, 6649-6664.

Wang, J., 2007a. Cohesive-bridging zone model of FRP-concrete interface debonding. Eng. Fracture Mech. 74, 2643-2658.

Wang, J., 2007b. Cohesive zone model of FRP-concrete interface debonding under mixed-mode loading. Int. J. Solids Structures 44, 6551-6568.

Wheat, D.L., 1994. Nonlinear analysis of two-layered wood members with interlayer slip. J. Struct. Eng. 120, 1909-1929.

Xu, R., Wu, Y., 2007. Static, dynamic and buckling analysis of partial interaction composite members using Timoshenko's beam theory. Int. J. Mech. Sciences 49, 1139-1155.